Journal of Hazardous Materials 193 (2011) 37–44

Contents lists available at ScienceDirect

Journal of Hazardous Materials

journal homepage: www.elsevier.com/locate/jhazmat

Optimization of complex conditions by response surface methodology for APAM–oil/water emulsion removal from aqua solutions using nano-sized TiO_2/Al_2O_3 PVDF ultrafiltration membrane

X.S. Yi [a], W.X. Shi [a], S.L.Yu [a,b,*], C. Ma [a], N. Sun [a], S. Wang [a], L.M. Jin [a], L.P. Sun [c]

[a] State Key Laboratory of Urban Water Resource and Environment, Harbin Institute of Technology, Harbin 150090, China
[b] State Key Laboratory of Pollution Control and Resources Reuse, Tongji University, Shanghai 200092, China
[c] Tianjin Key Laboratory of Aquatic Science and Technology, Tianjin Institute of Urban Construction, Tianjin 300384, China

ARTICLE INFO

Article history:
Received 30 March 2011
Received in revised form 18 June 2011
Accepted 23 June 2011
Available online 29 June 2011

Keywords:
Optimization
Complex conditions
Response surface methodology
APAM/oil/water emulsion
Ultrafiltration

ABSTRACT

This paper studies the cumulative effect of various parameters, namely anionic polyacrylamide (APAM) concentration, oil concentration, pH, trans-membrane pressure (TMP), and total dissolved solid (TDS), and obtains optimal parameters for the minimum relative flux (J/J_0) declining in aqueous solutions with response surface methodology (RSM). In order to analyze the mutual interaction and optimal values of parameters affecting ultrafiltration, a central composite rotatable design (CCRD), one method of RSM, was employed. The analysis of variance (ANOVA) of the cubic polynomial model demonstrated that this model was highly significant and reliable. The results show that the effect of APAM and oil on J/J_0 has an inverse trend with pH value increasing. Moreover, the mutual interaction of initial APAM (oil) concentration ($C_{APAM(oil)}$) and pH (TMP) were negligible, while the mutual interaction of C_{APAM} and C_{oil} has an obvious effect, i.e. the effect of initial feed C_{APAM} became more important at higher values of initial feed C_{oil}, and the J/J_0 was only about 4%. The favorable operate conditions in this ultrafiltration process were at low C_{APAM}, C_{oil}, pH, and TMP, which agreed with the conclusions of many authors, while considering water production, C_{APAM} and C_{oil} < 50 mg/L, pH < 4, and TMP < 0.075 MPa could be accepted.

1. Introduction

More and more synthetic big molecular weight polyacrylamides, especially anion polyacrylamides (APAM) are used in the oil field industry to enhance oil recovery in recent years [1]. At the same time, the co-production of significant quantities of wastewater containing APAM and oil/water emulsion appeared. Such wastewater must be treated before released into the environment, otherwise, the high organic content may severely pollute estuaries, rivers, lakes, soil, and even the air [2,3]. Thus, it is indispensable to treat APAM–oil/water wastewaters prior to their discharge to the environment. The use of membrane technology offers a potential method to deal with the submicron and micron sized oily wastewater because the porous membrane matrix can promote coalescence of micron and submicron oil droplets into larger ones that can be easily separated by gravity [4]. Several kinds of membrane processes including ultrafiltration [5], nanofiltration, and reverse osmosis [6] have been recently employed for oil/water separation and proved to be efficient. Among all these efficient methods, UF membrane technology has the higher efficiency and lower energy cost, which has been widely used in the process of emulsions separation, recently [7].

However, fouling is one of the main disadvantages in membrane separation process whenever long-term operation with proper efficiency is considered [8]. As we all know, this case can be proved by: (1) relative flux decline in constant pressure filtration; or (2) trans-membrane pressure (TMP) increase in constant flux filtration. Membrane fouling is basically responsible for the loss of membrane permeability or the increase of TMP, which increases the operation cost and requires frequent membrane cleaning or replacement. Therefore, it continues to be a vexing issue for membrane users [9]. In general, when membrane fouling takes place with macromolecules such as protein, PAM, and oil emulsions, which make the whole process inefficient and less feasible in terms of cost [10]. So far, many researches have been carried out on membrane fouling by oil/water emulsion [11,12], and some other investigations [13,14] concerning the effects of protein on membrane fouling. All of them had shown that fouling was mainly affected by the

* Corresponding author at: State Key Laboratory of Urban Water Resource and Environment, Harbin Institute of Technology, Harbin 150090, China.
Fax: +86 0454 86284101.
E-mail address: hityushuili@163.com (S.L.Yu).

0304-3894/$ – see front matter © 2011 Elsevier B.V. All rights reserved.
doi:10.1016/j.jhazmat.2011.06.063

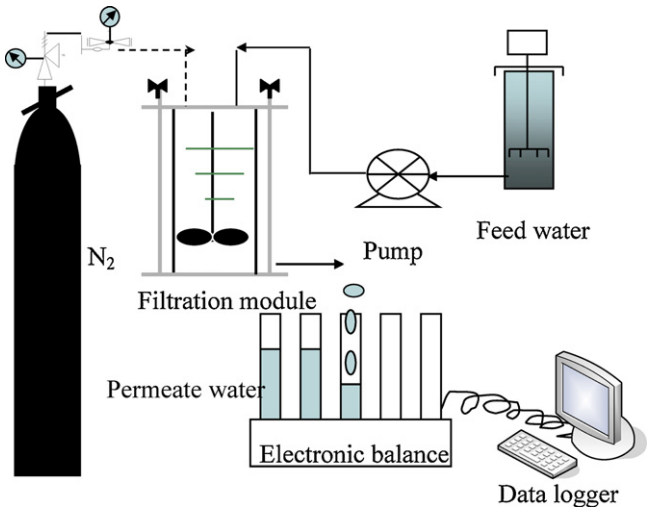

Fig. 1. Schematic diagram of experimental set-up for constant flux dead-end ultrafiltration.

pollutants–membrane interaction, operating parameters and the modules' design. However, few studies were performed on UF membrane fouling by polyelectrolyte and oil/water emulsion.

Almost all of the previously published research papers on dead-end ultrafiltration adopted the conventional experiment methods, which means one parameter varies while the others keep constant. In general, such conventional methods of experiments involve too many time-consuming experimental runs, but ignore interactions effects between the considered parameters of the process, leading to low efficiency in optimization issues [15].

Recently, response surface methodology (RSM) has been proved to be effective tools for investigation, modeling and optimization of the enhanced ultrafiltration processes. Xiarchos et al. [15] have applied RSM as the experimental approach on micellar-enhanced ultrafiltration in the study of separation of copper from aqueous solutions. Aydiner et al. [16] have applied the Taguchi experimental design to investigate the influence of factors upon on nickel rejection, surfactant rejection and steady-state flux in a surfactant-added powdered activated carbon/microfiltration hybrid process. The present work deals with the application of RSM tools for modeling and optimization of the effect of APAM–oil/water to relative flux decline in ultrafiltration process. The purpose of this dead-end ultrafiltration experiments was to optimize the complexation conditions in order to ensure the minimum flux ratio decline. The optimum conditions will be applied in real ultrafiltration systems operating in cross-flow mode.

2. Materials and methods

2.1. Apparatus

The schematic diagram of the experimental set-up (Fig. 1) used in our study was similar to those described in previous papers [17,18]. This system contained a dead-end stirred filtration cell (XFUF 07601, Millipore Co., U.S.A.) with a volume capacity of 300 mL, inner diameter of 76 mm, and effective area of membrane was 40 cm^2. All the UF experiments were carried out under certain TMP with extra nitrogen gas as pressed force, at a stirring speed of 100 rpm, under room temperature of $25 \pm 1\,^{\circ}C$. The Al_2O_3/TiO_2 PVDF UF membranes used here with nominal molecular weight limit (NMWL) 100 kDa (made in our laboratory) were prepared by the phase-inversion method. The casting solution was prepared by dissolving PVDF (19%, by weight of the solution) in the solvent (DMAC) at room temperature and adding nano-sized Al_2O_3, TiO_2 particles (0.19%, 0.38%, respectively) and PVP (4%) to the casting dopes while stirring. Then, the casting solution was scraped on glass plate by blow film machine, and placed into ethanol/water coagulation bath. Thus, the membranes were got. Each membrane was initially compacted for 0.5 h at 0.2 MPa higher than the highest operating pressure to prevent any possibility of change in membrane hydraulic resistance during UF [19,20]. The distance from the membrane surface to the top of the solution was 60 ± 2 mm, so the volume of solution in the cell was large enough to guarantee that concentration changed inside the cell would only take place near the membrane. Therefore, far from the membrane surface, the bulk concentration (C_0) remained unchanged during the process. Moreover, in order to ensure the validity of experiments, each membrane was used only once and discarded.

2.2. Chemicals

All chemicals involved in the experiments were of analytical grade. The solutions of APAM–oil/water were prepared using ultrapure deionized water from a Milli-Q system (Millipore, Bedford, U.S.A.). All glasswares were washed carefully with 2 M nitric acid and deionized water [21]. Crude oil from Daqing oil-filed as base oil, anionic surfactant (sodium dodecylsulfate, 98%, Tianjin); APAM (≥98.5%) from Daqing oil field in China was used to prepare stock APAM solutions (5000 mg/L) and feed APAM solutions (0 and 200 mg/L). The feed solutions were supplemented with $MgCl_2{\cdot}6H_2O$, $CaCl_2$, NaCl (1:1:1) to maintain total dissolved solid (TDS) at 0–8000 mg/L; 5 N NaOH and 5 N HNO_3 were used for pH adjustment. The selection of all these parameters based on different effluent qualities after different pretreatments.

2.3. Water quality analysis

Water quality was assessed by testing the feed and permeation water of this UF process. Oil and APAM content was analyzed by a UV spectrophotometer [12] (UV2550, Shimadzu, Japan); Table 1 shows the retention ratio of APAM and oil droplets of the two kinds of membranes under different conditions. APAM and oil retention ratio of the two membranes were all higher than 97%, and about 100%, respectively, thus, it was not necessary to consider APAM (oil) retention ratio and permeate residuals when relative flux decline was investigated in this study.

2.4. Relative flux decline studies

To investigate the effect of APAM–oil/water solution on relative flux decline of this UF process, flux was calculated every 2 min until it was stable (60 min). Pure water flux of this membrane was measured under the same condition with pure water determined by

Table 1
The rejection ratio of APAM and oil.

Rejection (%)	APAM (oil) (mg/L)			pH			TMP (MP)		
	20	100	200	3	6.8	10	0.05	0.10	0.20
APAM	97.5	99.8	99.7	98.6	98.8	98.2	98.8	97.4	97.3
Oil	100	100	100	100	100	99.9	100	100	99.8

Table 2
Code and level of factors chosen for the trial.

Variables	Symbols	Actual values of coded levels				
		$-\alpha$ (−2.00)	−1.00	0.00	1.00	$+\alpha$ (2.00)
APAM (mg/L)	X_1	0	50	100	150	200
Oil (mg/L)	X_2	0	50	100	150	200
pH	X_3	1	4	7	10	13
TMP (MPa)	X_4	0.05	0.075	0.10	0.125	0.15
TDS (mg/L)	X_5	0	2000	4000	6000	8000

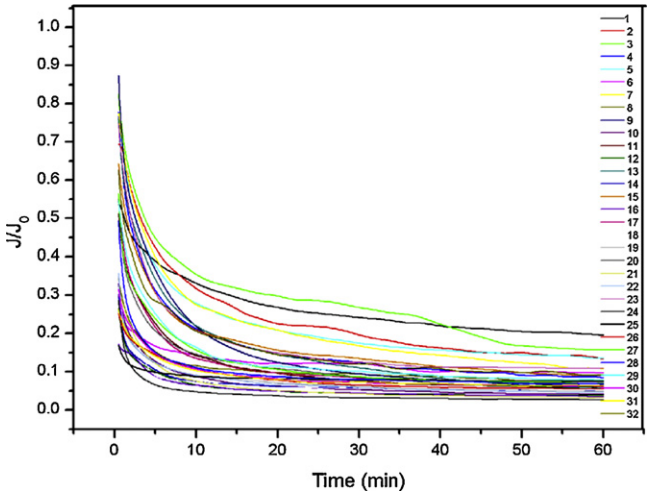

Fig. 2. Permeate flux ratio decline of J/J_0 versus time of the 32 experimental runs.

collecting permeating flux weight for 2 min, and we called this initial flux J_0. The range of variation of this J_0 was 100–120 L/m^2 h at 0.07 MPa, and 380–410 L/m^2 h at 0.2 MPa, respectively.

As the initial flux of every membrane was not quite the same, Relative flux (J/J_0, %) was adopted to evaluate the flux decline. The calculating equation was:

$$\frac{J}{J_0} = \frac{(m/\rho)/(A \cdot \Delta t)}{(m_w/\rho_w)/(A \cdot \Delta t)} = \frac{m}{m_w} \quad (1)$$

where m and m_w was the solution and pure water permeate weight, respectively (kg), A was the effective membrane area (m^2), Δt was the experimental time (min); ρ_w was the density of pure water, and $\rho_w = \rho$ could be used for the concentration of APAM and oil in permeate were all lower than 5 mg/L.

3. Results and discussion

3.1. Design of experiments and response surface modeling

Five process variables were chosen in the experimental design used for response surface modeling, namely: feed concentration of APAM (mg/L) and oil emulsion (mg/L), pH of feed solution, TMP (MPa), and TDS (mg/L).

Central composite rotatable designs (CCRD) are widely used in statistical modeling to obtain response surface models that set the mathematical relationships between response and variables [22]. In this paper, experiments were based on half central composite

Table 3
Experimental matrix and results of CCRD.

Standard order	Run order	APAM	Oil	pH	TMP	TDS	Response
1	9	−1.00	−1.00	−1.00	1.00	−1.00	6.4002
2	10	1.00	−1.00	−1.00	1.00	1.00	4.0968
3	21	0.00	0.00	−2.00	0.00	0.00	3.2002
4	11	−1.00	1.00	−1.00	1.00	1.00	6.0401
5	13	−1.00	−1.00	1.00	1.00	1.00	5.663
6	15	−1.00	1.00	1.00	1.00	−1.00	8.9557
7	2	1.00	−1.00	−1.00	−1.00	−1.00	13.2886
8	22	0.00	0.00	2.00	0.00	0.00	4.4999
9	6	1.00	−1.00	1.00	−1.00	1.00	9.605
10	32	0.00	0.00	0.00	0.00	0.00	9.2639
11	19	0.00	−2.00	0.00	0.00	0.00	4.7815
12	16	1.00	1.00	1.00	1.00	1.00	3.5002
13	17	−2.00	0.00	0.00	0.00	0.00	6.7885
14	1	−1.00	−1.00	−1.00	−1.00	1.00	19.503
15	20	0.00	2.00	0.00	0.00	0.00	5.5592
16	3	−1.00	1.00	−1.00	−1.00	−1.00	15.6422
17	14	1.00	−1.00	1.00	1.00	−1.00	4.857
18	26	0.00	0.00	0.00	0.00	2.00	5.5001
19	18	2.00	0.00	0.00	0.00	0.00	4.7306
20	8	1.00	1.00	1.00	−1.00	−1.00	7.6501
21	28	0.00	0.00	0.00	0.00	0.00	6.7638
22	24	0.00	0.00	0.00	2.00	0.00	2.6001
23	4	1.00	1.00	−1.00	−1.00	1.00	8.3846
24	7	−1.00	1.00	1.00	−1.00	1.00	10.7317
25	29	0.00	0.00	0.00	0.00	0.00	7.7714
26	23	0.00	0.00	0.00	−2.00	0.00	10.8999
27	5	−1.00	−1.00	1.00	−1.00	−1.00	13.4093
28	25	0.00	0.00	0.00	0.00	−2.00	7.3999
29	30	0.00	0.00	0.00	0.00	0.00	6.2371
30	31	0.00	0.00	0.00	0.00	0.00	6.2837
31	12	1.00	1.00	−1.00	1.00	−1.00	3.7998
32	27	0.00	0.00	0.00	0.00	0.00	7.0653

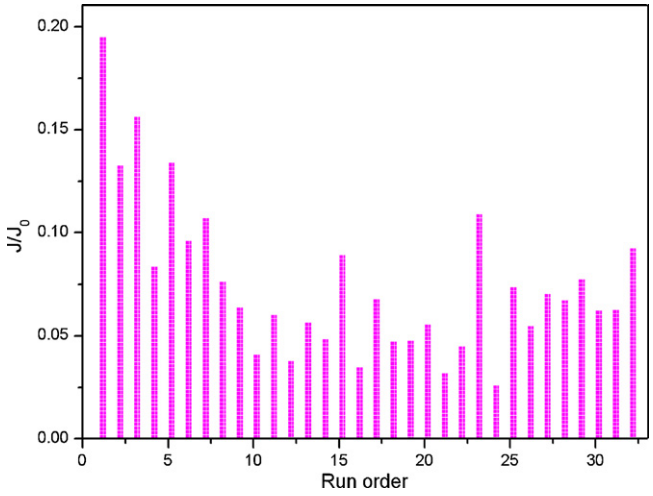

Fig. 3. Permeate flux ratio decline of J/J_0 at 60 min of the 32 experimental runs.

rotatable design (CCRD) with all combinations of the five factors at three levels: high (+1), low (−1), the center points (basic level, 0), which were the midpoints between the high and low levels, and were repeated six times. The start point ($\pm\alpha$) which was set at the outer value corresponding to a value of ±2. Five process variables involved in the study are shown in Table 2. The design matrix of coded values for the factors and the response in terms of J/J_0 for all experimental runs (taking the average value of three parallel experiments) generated by the Expert Designer software is shown in Table 3.

The experimental data of J/J_0 were plotted versus time are shown in Fig. 2. These curves represented the evolution of permeate flux decline with time, with a shape composed by two regions:

Table 4
ANOVA table (partial sum of squares) for adjust cubic model (response: J/J_0).

Source	SS	DF	MS	F	P
Model	306.86	8	38.36	6.39	0.0002
Residual error	138.07	23	6.00		
Lack-of-fit	131.51	18	7.31	7.31	5.57
Pure error	6.56	5	7.31	1.31	
Total	444.93	31			

the first stage was J/J_0 declines sharply, the second stage was J/J_0 declines slowly until a relative stationary permeate flux reached. Fig. 3 indicates that the permeate relative flux decline of J/J_0 at 60 min after stability of these 32 experimental runs.

Generally, a second-order polynomial model with main, quadratic and interaction terms can be developed to fit the experimental data obtained from the experimental runs conducted on the basis of CCRD [23,24]. However, it was not enough to evaluate this UF process for there were too many factors (five main factors). Thus, a third-order polynomial model with main, quadratic, cubic, and interaction terms was used in this study. The RSM, known as regression or empirical equation, represents an approximation of experimental data and is stated by the following relationship:

$$y = b_0 + \sum_{i=1}^{n} b_i x_i + \sum_{i=1}^{n} b_{ii} x_i^2 + \sum_{i=1}^{n} b_{iii} x_i^3 + \sum_{i=1}^{n-1} \sum_{j=i+1}^{n} b_{ij} x_i x_j + \sum_{i=1}^{n-2} \sum_{j=i+1}^{n-1} \sum_{k=i+2}^{n} b_{ijk} x_i x_j x_k + \sum_{i=1}^{n-1} \sum_{j=i+1}^{n} b_{iij} x_i^2 x_j \quad (2)$$

where y is the predicted response (J/J_0), X_i, X_j, X_k refers to the coded levels of the design variables, b_0 the constant coefficient, b_i linear coefficients, b_{ii} quadratic coefficients, b_{ij}, b_{iik} and b_{iij} the interaction coefficients, b_{iii} cubic coefficients, and u number of design

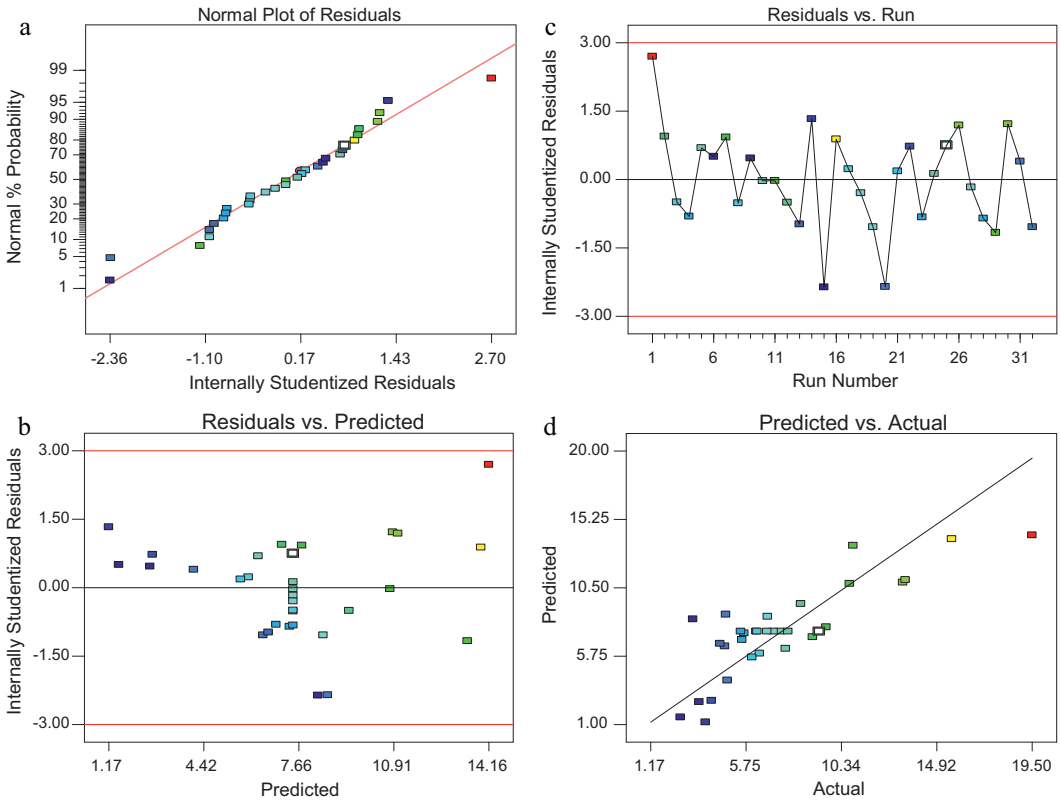

Fig. 4. Residuals plots (a, b, and c) for the CCRD design and the relationship of predicted and actual value (d).

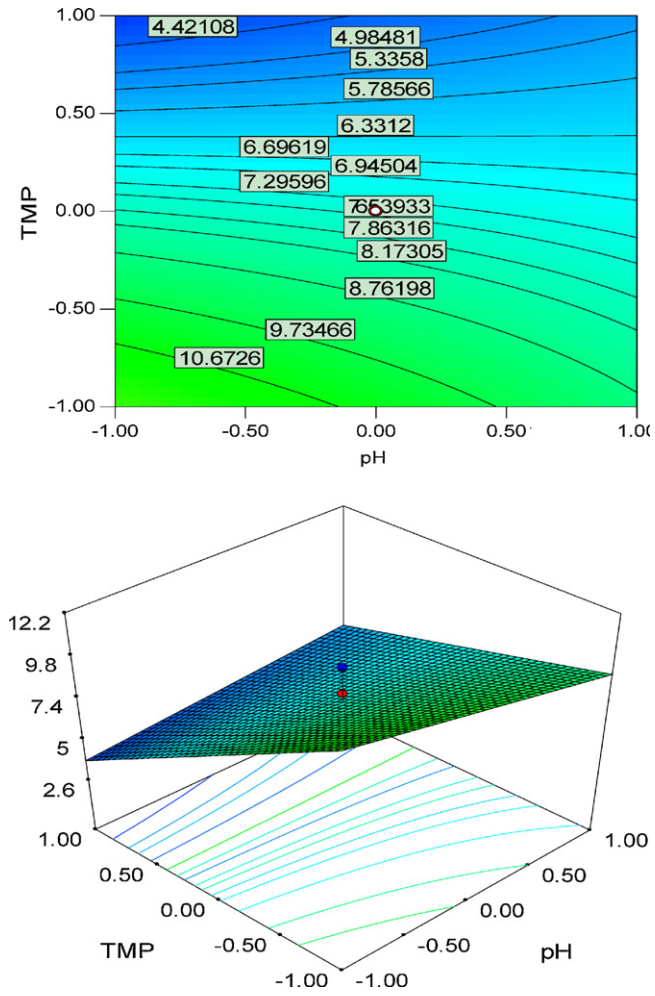

Fig. 5. Permeate flux ratio decline (J/J_0) surface plot and contour-lines map depending on TMP and pH variables, holding the other variable at its center level.

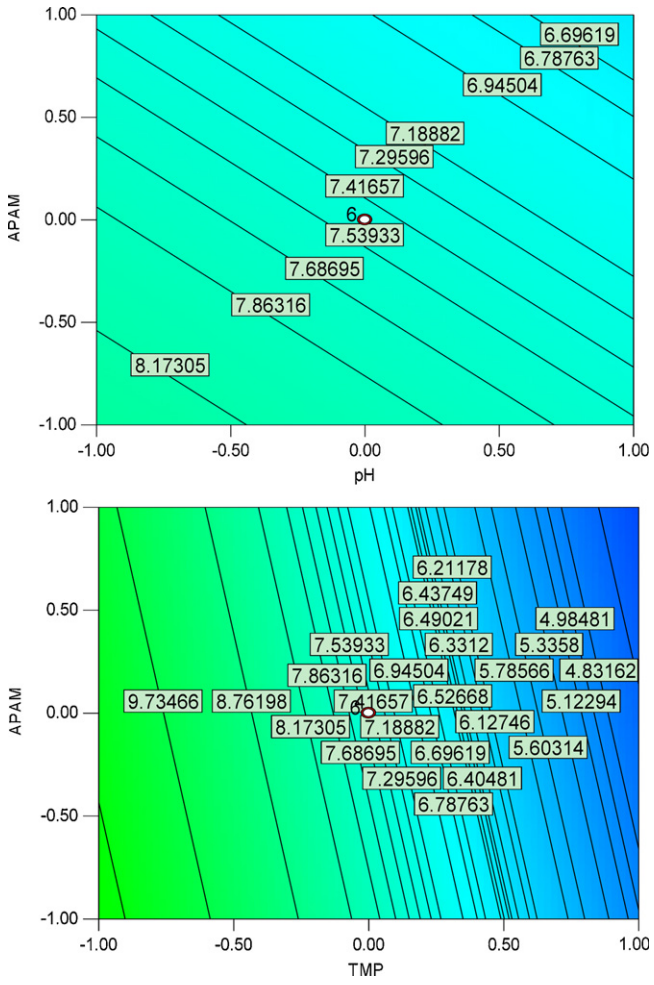

Fig. 6. Contour-line plots of permeate flux ratio decline depending on APAM feed concentration (C_{APAM}) and pH (TMP) variables, holding the other variable at its center level.

variables. The least square estimations of the regression coefficients have been computed by means of multiple linear regression (MLR) method. The validity of the cubic empirical model was tested with analysis of variance (ANOVA) with the confidence level 95%.

3.2. ANOVA analysis for ultrafiltration of APAM–oil/water emulsion

In order to ensure a good model, the test for significance of the regression model was performed applying the analysis of variances (ANOVA). Table 4 shows the relationships used for calculation of the ANOVA estimators at 95% confidence level, which were widely presented in the literature concerning RSM [25].

The significance of the model was determined by Fisher test [26]. The model *F*-value of 6.39 and *P*-value of 0.0002 implied the model was significant. And there was only a 0.02% chance that an error could occur due to noise. All these statistical estimators revealed that the response model could be accepted from statistical point of view for the prediction of the response in the considered range of factors (valid regions). According to Student's *t*-test, the smaller the *P*-value, the more significant of each coefficient [27], thus, the order of those significant factors in this study was as follows:

X_4: TMP, first order main effect; > X_3X_4: interaction of pH and TMP; > $X_1X_2^2$: interaction of concentration of APAM and quadratic of concentration of oil; > X_2: concentration of oil, first order main effect; > X_3: pH, first order main effect; > X_1: concentration of APAM, first order main effect; > X_1X_2: interaction of concentration of APAM and concentration of oil; > X_2^2: quadratic main effect of concentration of oil.

Thus, a cubic regression model with coded variables for flux ratio decline (J/J_0) was developed based on experimental design.

$$y = 7.4713 - 0.5145x_1 - 0.4401x_2 - 0.4243x_3 - 2.9792x_4 - 0.3067x_1x_2 + 1.1288x_3x_4 + 0.0745x_2^2 - 1.4332x_1x_2^2 \quad (3)$$

subjected to: $-\alpha \le X_i \le \alpha$, for $i = 1, 2, 3, 4, 5$.

After variables naturalization, which meant normalized variables replaced by natural variables, regression model of natural variables was built as the following:

$$y = 32.7449 - 0.00653C_{APAM} - 0.01954C_{oil} - 1.6465\text{pH} - 224.523\text{TMP} - 4.78 \times 10^{-5}C_{APAM} \cdot C_{oil} + 15.0507\text{pH} \cdot \text{TMP} + 1.15 \times 10^{-4}C_{oil}^2 - 8.5417 \times 10^{-7}C_{APAM} \cdot C_{oil}^2 \quad (4)$$

subjected to: $0 \le C_{APAM} \le 200$ (mg/L); $0 \le C_{oil} \le 200$ (mg/L), $1 \le \text{pH} \le 13$; $0.05 \le \text{TMP} \le 0.15$ (MPa).

This model can be used to predict the relative flux decline of APAM–oil/water emulsion within the limits of experimental parameters. The plot of the residuals normal probability and the residuals versus the predicted response are shown in Fig. 4. It was observed in Fig. 4(a) that, the residuals generally fall on a straight line, implying that errors are distributed normally, and thus, support adequacy of the least-square fit [26]. Moreover, residuals are equally scatter above and below the *x*-axis with no obvious pattern

and unusual structure, and all these points are less than ±3.00 (Fig. 4(b) and (c)), which implies that the model proposed was adequate and reliable. Thus, there was no reason to suspect any violation of the independence or constant variance assumption. Fig. 4(d) shows us the relationship of predicted and experimental results. It can be seen from Fig. 4(d) that the response model showed a goodness of fit to the experimental data in different conditions, because there was only a few actual points has obvious discrepancy with the predicted values, and its predict R^2 0.8545. Therefore, the model was considered adequate for the prediction and optimization of flux ratio decline.

3.3. The effects of factors on permeate flux ratio decline (J/J_0)

The contour and surface plots of the response functions are useful in understanding both the main and the interaction effects of the factors. These plots can be obtained by computations using the developed response models and adequate software—Design Expert.

3.3.1. Effect of TMP and pH

Fig. 5 shows the predicted permeate relative flux (J/J_0) decline, spanned by pH and TMP. It was observed that, TMP has a significant negative effect on J/J_0 decline. For example, the permeate flux increased when increasing the driving force (TMP), however, the permeate relative flux declined obviously, which means the membrane fouling was more serious. The reason was that a layer containing large oil droplets starts forming just above the membrane surface which may be compressed on the surface and blocked the membrane pores at high TMP, leading to membrane fouling at a higher rate [28,29]. Moreover, APAM was another factor which caused the relative flux decline decreased sharply. The reason was that high TMP might press the APAM molecule and cause radius decreasing [30], then pushed and delivered more APAM molecules into membrane pores resulting in severe inner pore adsorption/clogging.

PH value is another important parameter to take into account in the formation of the macromolecular complexes for APAM and oil [31]. It can be seen from Fig. 5 that, the contour lines are slight curvatures, implying there has an interaction between pH and TMP. TMP played a determinant role, the higher the pH, the lower of J/J_0, only 5.8% at pH 4 when TMP above 0.125 MPa; while J/J_0 (10.6%, pH 4) increased with pH value decreasing when TMP lower than 0.125 MPa. The reason was that the gyration radius of APAM increased with pH increasing, while induced the smaller oil droplets formation. Therefore, although the gyration radius of APAM were bigger at higher pH, membrane pores were easily blocked with oil droplets and the APAM molecular compressed by the high TMP; While, when the TMP was low, it was still hard to force the APAM molecular which had smaller gyration radius with low pH into pores, thus the membrane fouling decreasing. Above all, the interaction of TMP (which has a negative effect) and pH which has a complex effect on permeate flux ratio decline, caused the contour lines curved.

3.3.2. Effect of APAM and oil feed concentration

In Figs. 6–8 the response surfaces plots and contour-lines maps are presented for the permeate relative flux (J/J_0) decline predicted function revealing the influence of factors (design variables) upon the investigated responses. The contour line maps illustrated in Figs. 6 and 7 indicating that the increasing of both pH and APAM (oil) lead to J/J_0 decreasing, while the other three factors were all at their central level. Fig. 6 shows that there was no obvious interaction effects between APAM feed concentration (C_{APAM}) and pH (TMP), because all of these contour lines are straight. Thus, an optimal region where the response remains at maximal level can be seen in the range of pH <4; C_{APAM} <50 mg/L; TMP <0.075 MPa. Similarly,

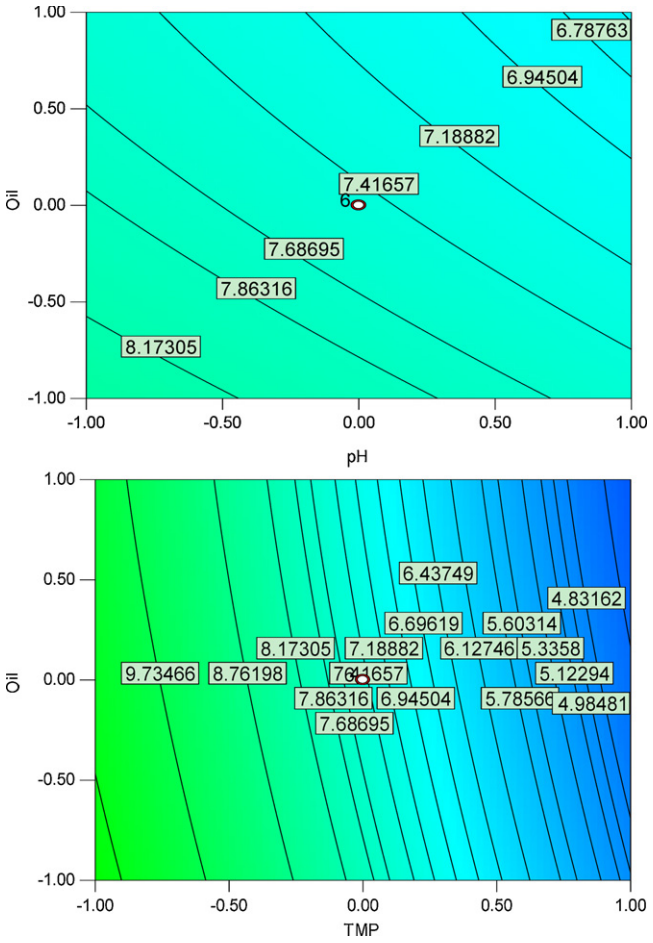

Fig. 7. Contour-line plots of permeate flux ratio decline depending on oil feed concentration (C_{oil}) and pH (TMP) variables, holding the other variable at its center level.

although there has a small interaction effect between oil feed concentration (C_{oil}) and pH (TMP) shown in Fig. 7, this interaction could be neglected, and the optimal region can be achieved in the range of pH < 4; C_{oil} < 50 mg/L; TMP < 0.075 MPa. This could be explained by electrostatic interaction between the membrane surface and the oil droplets under different pH values [32].

The interaction effect of initial APAM (oil) concentration and pH or TMP are negligible (Figs. 6 and 7), while the interaction between initial APAM concentration and initial oil concentration has an obvious effect (Fig. 8). For instance, the effect of initial feed C_{APAM} becomes more important at higher values of initial feed C_{oil}, and the relative flux J/J_0 was only about 4%, while at lower values of initial feed C_{oil}, the J/J_0 could reach to about 9% (Fig. 8). Moreover, the contour lines were curves with oil concentration increasing, which was mainly caused by the interaction of oil and APAM. Thus, permeate relative flux decreased sharply caused by the increasing in the APAM feed concentration, and this could be explained by the increasing of the viscosity of the adhesion from the macromolecular polymer (APAM), then the corresponding macromolecular took up a tightly packed conformation [33], in addition, concentration polarization phenomenon was enhanced by a high APAM feed concentration [34,35]. However, Chakrabarty et al. [11] reported that as oil concentration increases, relative flux decreases sharply for the formation of thicker oil layer on the membrane surface. In this paper, the effect of oil droplets was not as obvious as we expected. The reason was that oil droplets were embedded by APAM colloid, and APAM molecular played a determined role in membrane fouling. Further more, the nano-sized TiO_2/Al_2O_3 in PVDF membrane

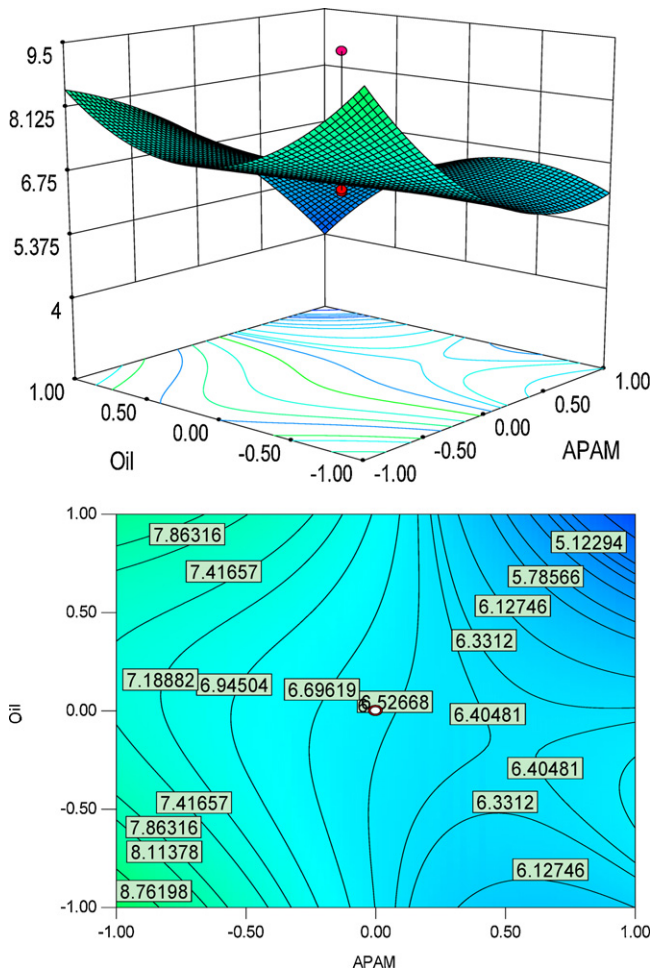

Fig. 8. Permeate flux ratio decline (J/J_0) surface plot and contour-lines map depending on C_{APAM} and C_{oil}, holding the other variable at its center level.

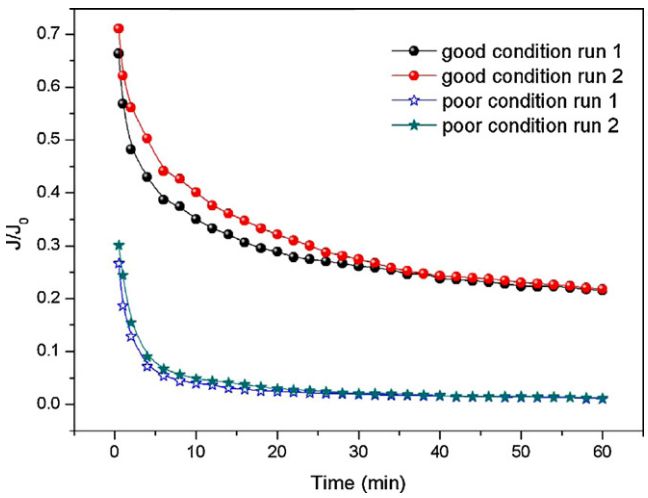

Fig. 9. Permeate flux ratio decline of J/J_0 versus time in two typical conditions. Good condition: oil and APAM 20 mg/L, pH 2, TMP 0.05 MPa; poor condition: oil and APAM 200 mg/L, pH 12, TMP 0.15 MPa.

prevented the oil droplets from adsorbing on the membrane surface, but can be adsorbed by hydrophilic APAM for the hydrophilic properties [36].

3.4. The ultrafiltration process optimization testing

According to the results about parameters optimization process, an ultrafiltration process optimization testing has done to verify the validity of statistical methods. Fig. 9 presents the permeate flux with time plot for the typical superior and poor conditions of this UF process.

From the figure it is observed that low concentration of oil and APAM at 20 mg/L, low pH 2, with low TMP 0.05 MPa can give a steady relative flux value of 21.51% at 60 min. On the contrary, at a concentration of 200 mg/L, pH 12, and TMP 0.15 MPa, the relative flux value of at 60 min was only about 0.105%. Moreover, the two flux ratio values of the two UF processes calculated by the predicted model were 19.34% and −2.95%, respectively, which are very similar with the experimental values. This result showed that the regression model was very effective in predicting flux ratio of this process, and also revealed that the optimal operation parameters were: low concentration of organic matters, low pH, and low TMP. Of cause, not all of these parameters are suitable for practical use, because water production should be another important factors need to be considered except antifouling characteristics we studied here. Therefore, it was necessary to have an appropriate pretreatment in front of this UF process, because with the dilution, a lower TMP could achieve higher average permeate flux, exhibiting less formation of concentration boundary layer, i.e. less membrane fouling on the membrane surface. Moreover, the process become more economical in terms of energy consideration and also dilution imparts a favorable impact on the reusability and longevity of the membrane.

4. Conclusions

Response surface methodology (RSM) and the central composite rotatable design (CCRD) have been proved to be important tools in studying the effect of process factors on permeate flux ratio decline from aqueous solutions via ultrafiltration. It was found that among the five process factors considered (namely, APAM concentration, oil concentration, pH, TMP, and TDS), TMP, oil and APAM concentration had significant effect on the permeate relative flux (J/J_0) decline using of CCRD and multiple regression method. The effect of TMP was to deform APAM and oil molecule, then, compress them on the surface and block the membrane pores. In addition, the effect of C_{APAM} and C_{oil} at different pH was observed: the higher the pH value, the more serious membrane fouling was got. Moreover, it was found that the interaction effect of initial C_{APAM} (C_{oil}) and pH or TMP are negligible, while the interaction between initial C_{APAM} and C_{oil} has an obvious effect, i.e. the effect of initial feed C_{APAM} becomes more important at higher values of initial feed C_{oil}, and the J/J_0 was only about 4%, while at lower values of initial feed C_{oil}, the J/J_0 could reach to about 9%. The favorable operate conditions in this ultrafiltration process were at low C_{APAM}, C_{oil}, pH, and TMP, which agreed with the conclusions of many authors, while considering water production, C_{APAM} and C_{oil} < 50 mg/L, pH < 4, and TMP < 0.075 MPa could be accepted. Thus, RSM methodology could be successfully used to study the importance of the effects of process variables and find the optimal operation ozone in ultrafiltration.

Acknowledgements

The authors gratefully acknowledge the financial support provided by the National Science Foundation (Grant: 50978068); State water pollution control and harnessing of the major projects (2009ZX07424-005); State key Lab of Urban Water Resource and Environment (HIT) (Grant No. 2008QN05); and Tianjin Key Laboratory of Aquatic Science and Technology, Tianjin Institute of Urban

Construction. The authors also acknowledge State Key Laboratory of Urban Water Resource and Environment, Harbin Institute of Technology for their support during the conduct of this research.

References

[1] X. Zhao, L. Liu, Y. Wang, H. Dai, D. Wang, H. Cai, Influences of partially hydrolyzed polyacrylamide (HPAM) residue on the flocculation behavior of oily wastewater produced from polymer flooding, Sep. Purif. Technol. 62 (2008) 199–204.
[2] Z. Chen, G.H. Huang, J.B. Li, A GIS-based modeling system for petroleum waste management, Water Sci. Technol. 47 (2003) 309–317.
[3] S.F.V. Jerez, J.M. Godoy, N. Miekeley, Environmental impact studies of barium and radium discharges by produced waters from the "Bacia de Campos" oil-field offshore platforms Brazil, J. Environ Radioact. 62 (2002) 29–38.
[4] M. Hlavacek, Break-up of oil-in-water emulsions induced by permeation through a microfiltration membrane, J. Membr. Sci. 102 (1995) 1–7.
[5] M. Belkacem, M. Bahlouli, A. Mraoui, K. Bensadok, Treatment of oil–water emulsion by ultrafiltration: a numerical approach, Desalination 206 (2007) 433–439.
[6] P.H. Wolf, S. Siverns, S. Monti, UF membranes for RO desalination pretreatment, Desalination 182 (2005) 293–300.
[7] D.A. Masciola, R.C. Viadero Jr., B.E. Reed, Tubular ultrafiltration flux prediction for oil-in-water emulsions: analysis of series resistances, J. Membr. Sci. 184 (2001) 197–208.
[8] D. Sen, W. Roy, L. Das, S. Sadhu, C. Bhattacharjee, Ultrafiltration of macromolecules using rotating disc membrane module (RDMM) equipped with vanes: effects of turbulence promoter, J. Membr. Sci. 360 (2010) 40–47.
[9] X. Sun, D.M. Kanani, R. Ghosh, Characterization and theoretical analysis of protein fouling of cellulose acetate membrane during constant flux dead-end microfiltration, J. Membr. Sci. 320 (2008) 372–380.
[10] Y. Lu, J.R. Levick, W. Wang, Concentration polarization of hyaluronan on the surface of the synovial lining of infused joints, J. Physiol. 561 (2004) 559–573.
[11] B. Chakrabarty, A.K. Ghoshal, M.K. Purkait, Ultrafiltration of stable oil-in-water emulsion by polysulfone membrane, J. Membr. Sci. 325 (2008) 427–437.
[12] S.L. Yu, Y. Lu, B.X. Chai, J.H. Li, Treatment of oily wastewater by organic–inorganic composite tubular ultrafiltration (UF) membranes, Desalination 196 (2006) 76–83.
[13] X.H. Sun, D.M. Kanani, R. Ghosh, Characterization and theoretical analysis of protein fouling of cellulose acetate membrane during constant flux dead-end microfiltration, J. Membr. Sci. 320 (2008) 372–380.
[14] Q. Li, M. Elimelech, Organic fouling and chemical cleaning of nanofiltration membranes: measurements and mechanisms, Environ. Sci. Technol. 38 (2004) 4683.
[15] I. Xiarchosa, A. Jaworskab, G. Zakrzewska-Trznadel, Response surface methodology for the modeling of copper removal from aqueous solutions using micellar-enhanced ultrafiltration, J. Membr. Sci. 321 (2008) 222–231.
[16] C. Aydiner, M. Bayramoglu, S. Kara, B. Keskinler, O. Ince Nickel, Removal from waters using surfactant-enhanced Hybrid PAC/MF process. I. The influence of system-component variables, Ind. Eng. Chem. Res. 45 (2006) 3926–3933.
[17] J. Fernández-Sempere, F. Ruiz-Beviá, P. García-Algado, R. Salcedo-Díaz, Visualization and modeling of the polarization layer and a reversible adsorption process in PEG-10000 dead-end ultrafiltration, J. Membr. Sci. 342 (2009) 279–290.
[18] F. Ruiz-Beviá, J. Fernández-Sempere, R. Salcedo-Díaz, P. García-Algado, Diffusion studies in polarized reverse osmosis processes by holographic interferometry, Opt. Laser Eng. 46 (2008) 877–887.
[19] Y.L. Su, W. Cheng, C. Li, Z.Y. Jiang, Preparation of antifouling ultrafiltration membranes with poly (ethylene glycol)-graft-polyacrylonitrile copolymers, J. Membr. Sci. 329 (2009) 246–252.
[20] S. Mimoune, F. Amrani, Experimental, study of metal ions removal from aqueous solutions by complexation–ultrafiltration, J. Membr. Sci. 298 (2007) 92–98.
[21] J.A. Jurado-González, M.D. Galindo-Riaño, M. García-Vargas, Factorial designs applied to the development of a capillary electrophoresis method for the analysis of zinc, sodium, calcium and magnesium in water samples, Talanta 59 (2003) 775–783.
[22] C. Cojocaru, G. Zakrzewska-Trznadel, Response surface modeling and optimization of copper removal from aqua solutions using polymer assisted ultrafiltration, J. Membr. Sci. 298 (2007) 56–70.
[23] C. Cojocaru, G. Zakrzewska-Trznadel, A. Jaworska, Removal of cobalt ions from aqueous solutions by polymer assisted ultrafiltration using experimental design approach. Part 1: optimization of complexation conditions, J. Hazard. Mater. 169 (2009) 599–609.
[24] M. Martí-Calatayud, M. Vincent-Vela, S. Álvarez-Blanco, J. Lora-García, E. Bergantiños-Rodríguez, Analysis and optimization of the influence of operating conditions in the ultrafiltration of macromolecules using a response surface methodological approach, Chem. Eng. J. 156 (2010) 337–346.
[25] J. Landaburu-Aguirre, E. Pongrácz, P. Perämäki, R.L. Keiski, Micellar-enhanced ultrafiltration for the removal of cadmium and zinc: use of response surface methodology to improve understanding of process performance and optimization, J. Hazard. Mater. 180 (2010) 524–534.
[26] Minitab® Release 14, Design of Experiments, User's Manual, Minitab Inc., 2003.
[27] W.G. Cochran, G.M. Cox, Experimental Designs, 2nd ed., John Wiley & Sons, New York, 1992.
[28] A.B. Koltuniewiz, R.W. Field, Process factors during removal of oil-in-water emulsions with crossflow microfiltration, Desalination 105 (1996) 79–89.
[29] M.J. Um, S.H. Yoon, C.H. Lee, K.Y. Chung, K.Y. Kim, Flux enhancement with gas injection in crossflow ultrafiltration of oily wastewater, Water Res. 35 (2001) 4095–4101.
[30] A.A. McCarthy, P.K. Walsh, G. Foley, Experimental techniques for quantifying the cake mass, the cake and membrane resistances and the specific cake resistance during crossflow filtration of microbial suspension, J. Membr. Sci. 201 (2002) 31–45.
[31] S. Mimoune, F. Amrani, Experimental study of metal ions removal from aqueous solutions by complexation–ultrafiltration, J. Membr. Sci. 298 (2007) 92–98.
[32] A.J. Chhatre, K.V. Marathe, Dynamic analysis and optimization of surfactant dosage in micellar enhanced ultrafiltration of nickel from aqueous streams, Sep. Sci. Technol. 41 (2006) 2755–2770.
[33] N. Hojo, H. Shirai, S. Hayashi, Complex formation between poly(vinyl alcohol) and metallic ions in aqueous solution, J. Polym. Sci. Symp. (1974) 299–307 (47).
[34] K. Xu, G.M. Zeng, J.H. Huang, J.Y. Wu, Y.Y. Fang, G. Huang, J. Li, B. Xi, H. Liu, Removal of Cd^{2+} from synthetic wastewater using micellar-enhanced ultrafiltration with hollow fiber membrane, Colloids Surf. A 294 (2007) 140–146.
[35] G. Ghosh, P.K. Bhattacharya, Hexavalent chromium ion removal through micellar enhanced ultrafiltration, Chem. Eng. J. 119 (2006) 45–53.
[36] J. Zhou, Q. Chang, Y. Wang, J. Wang, G. Meng, Separation of stable oil–water emulsion by the hydrophilic nano-sized ZrO_2 modified Al_2O_3 microfiltration membrane, Sep. Purif. Technol. 75 (2010) 243–248.